Giant negative thermal expansion in La-doped CaFe_{2}As_{2}

A. Rebello, J. J. Neumeier, Zhaoshun Gao, Yanpeng Qi, and Yanwei Ma

Phys. Rev. B **86**, 104303 — Published 10 September 2012

DOI: 10.1103/PhysRevB.86.104303

Giant negative thermal expansion in La-doped $CaFe_2As_2$

A. Rebello and J. J. Neumeier
Department of Physics, P. O. Box 173840, Montana State University, Bozeman, MT 59717-3840, USA

Zhaoshun Gao, Yanpeng Qi, and Yanwei Ma
Key Laboratory of Applied Superconductivity, Institute of Electrical Engineering, Chinese Academy of Sciences, Beijing 100190, China
(Dated: June 26, 2012)

Lanthanum doping for calcium in $CaFe_2As_2$ results in negative thermal expansion that can be exceptionally large. The behavior is unusual among Fe-As materials, and is presumably associated with the close proximity of $CaFe_2As_2$ to a structural phase instability.

PACS numbers: 65.40.-b, 65.40.De, 63.20.Ry

I. INTRODUCTION

In the absence of thermodynamic phase transitions, most solids expand upon warming as a result of anharmonic contributions to the potential energy of the atoms.[1] However, some solids are known to contract upon warming, or in the case of anisotropic solids, to contract along some of the principal crystallographic axes upon warming.[2] Such behavior can be associated with unusual contributions to the potential energy or with atomic vibrational modes that are restricted to anisotropic solids.[2,3] However, contraction upon warming, known as negative thermal expansion (NTE), is generally rather small in magnitude for inorganic solids, and often occurs over a narrow temperature range. Here we reveal a solid, $Ca_{1-x}La_xFe_2As_2$ ($0.15 \leq x \leq 0.25$), that possesses an exceptionally large *and* negative volume thermal expansion comprised of an extraordinarily large and negative expansion along the crystallographic a-axis. The thermal expansion (TE) along the c-axis can be negative below ∼120 K, depending on the composition. Only polymers[4] and weakly bound solids such as xenon[1] exhibit volumetric TEs with comparable or larger magnitude. The results reveal unusual behavior of the thermal expansion in a metallic, inorganic solid that appears to be associated with strong coupling among the lattice, electronic, and magnetic degrees of freedom in the vicinity of a structural phase instability.

The tetragonal crystal structure of $CaFe_2As_2$ ($I4/mmm$) is characterized by Ca layers separating each Fe_2As_2 layer as shown in Fig. 1. Antiferromagnetic order is accompanied by a tetragonal-orthorhombic structural phase transition;[5] partial substitution of the rare earth ions La, Ce, Pr, or Nd for Ca suppresses the antiferromagnetic order and the structural transition.[6] Interlayer As-As bonding mediates formation of another tetragonal phase, known as collapsed tetragonal.[6,7] Modest external pressure[8] stabilizes this phase in $CaFe_2As_2$. Pr or Nd substitution stabilize it as well and also lead to superconductivity[6] at transition temperatures $T_c \leq 47$ K. For the La-doped samples, superconductivity occurs at[6,9] $T_c \leq 43$ K with no structural collapse.[6]

II. EXPERIMENTAL METHODS

Single crystals were grown in FeAs flux.[10] Analysis with a scanning electron microscope yielded the chemical compositions $Ca_{0.85}La_{0.15}Fe_2As_2$ ($3.45\times1.45\times0.2$ mm^3 along the planar directions and the c axis, respectively), $Ca_{0.80}La_{0.20}Fe_2As_2$ ($2.75\times1.85\times1.28$ mm^3), and $Ca_{0.75}La_{0.25}Fe_2As_2$ ($2.67\times2.00\times0.642$ mm^3). The crystallographic orientation was confirmed with Laue x-ray diffraction. Specific heat was measured using a Quantum Design PPMS. Expansion measurements utilized a fused-quartz dilatometer[11] with sensitivity to changes in length of 0.1 Å. This relative resolution is at least 1000x more sensitive than possible with diffraction techniques. Calibration was conducted using a sample of high-purity copper, which determines the *absolute* accuracy of the measured length changes as 0.24%. The samples were measured along two perpendicular directions in the a-b plane; both directions yielded identical behavior. Measurements along each axis were repeated 2-3 times. Each measurement curve consists of 1700 data points acquired while warming at 0.2 K/min. In calculating the thermal expansion coefficient along a short sample axis ($< 1mm$), a piece-wise Chebyshev polynomial fit of $\triangle L/L_{300}$ was performed before taking the point by point derivative. The thermal expansion coefficient derived from this fit was compared to that determined from taking the point by point derivative of the raw $\triangle L/L_{300}$ data to be certain that no small features were overlooked. $\triangle V/V_{300}$ was determined by adding twice $\triangle L/L_{300}$ along a to $\triangle L/L_{300}$ along c.

III. ELECTRICAL RESISTIVITY, MAGNETIC SUSCEPTIBILITY, AND HEAT CAPACITY

Electrical resistivity ρ was measured for the temperature range 2 K $< T <$ 300 K (see Fig. 2) in the plane of the platelet-like $Ca_{1-x}La_xFe_2As_2$ (x = 0.15, 0.20, and 0.25) single crystals (i.e. current was applied perpendicular to the c-axis, and the voltage drop was measured in the same plane). In the case of $Ca_{0.85}La_{0.15}Fe_2As_2$,

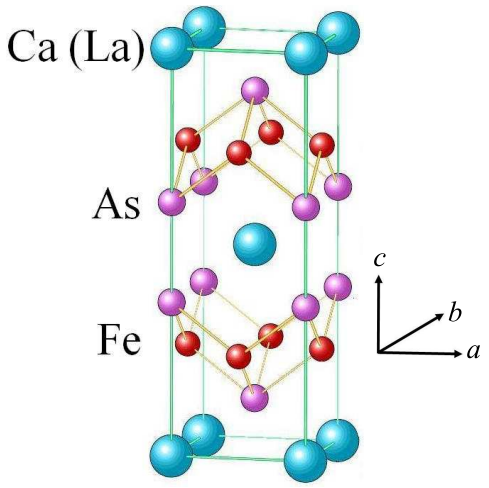

FIG. 1: (color online) Crystal structure of $Ca_{1-x}La_xFe_2As_2$.

values of $\rho(300K) = 751$ $\mu\Omega$ cm and $\rho(42.7K) = 142$ $\mu\Omega$ cm give a resistivity ratio $\rho_{300K}/\rho_{42.7K} = 5.2$. Thus, the temperature dependence is metallic, but the magnitude of ρ leads to classification as a poor metal (ρ is 20 to 300 times larger than in elemental metals). As x increases, the resistivity at 300 K also increases. All three samples exhibit a transition to superconductivity, but the transitions are broad due to an exceptionally small superconducting volume fraction (discussed below).

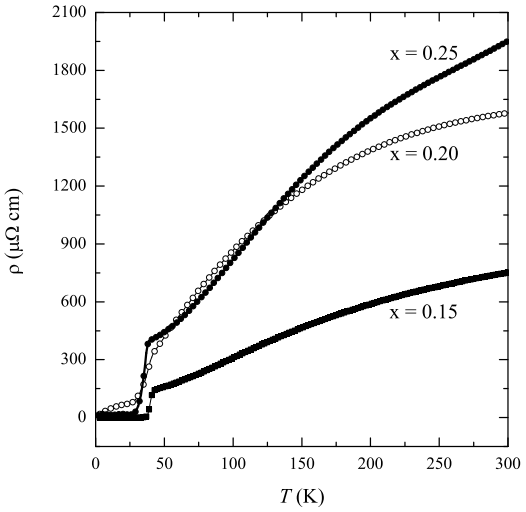

FIG. 2: Electrical resistivity ρ of the $Ca_{1-x}La_xFe_2As_2$ single crystals with x = 0.15, 0.20, and 0.25. Current was applied perpendicular to the c axis.

The magnetization M in an applied magnetic field of 1 tesla is shown in Fig. 3 for the magnetic field perpendicular to the c axis. $Ca_{0.85}La_{0.15}Fe_2As_2$ displays a very weak temperature dependence, and a diamagnetic transition below 20 K that is associated with superconductivity. Magnetic susceptibility measurements in an applied magnetic field of 10 mT were conducted under field cooled (FC) and zero-field cooled (ZFC) conditions. The diamagnetic signal confirms superconductivity, but the superconducting volume fraction obtained from the FC curve is only 0.02%, which shows that the sample is not a bulk superconductor. Minimal superconducting volume fractions were observed for x = 0.20 and 0.25 as well, and we therefore conclude that none of the samples studied herein are bulk superconductors. This conclusion is in agreement with others who have measured similar compositions.[6] M for x = 0.20 and 0.25 is larger in magnitude than is observed for x = 0.15. The temperature dependence seems to suggest the existence of local magnetic moments that increase in concentration with x. However, $1/\chi$ is linear only between 25 K and 100 K for both samples (χ is the magnetic susceptibility), which is not convincing evidence of Curie-Weiss behavior. There is a slight upturn below 140 K for x = 0.25 for which the origin is unclear.

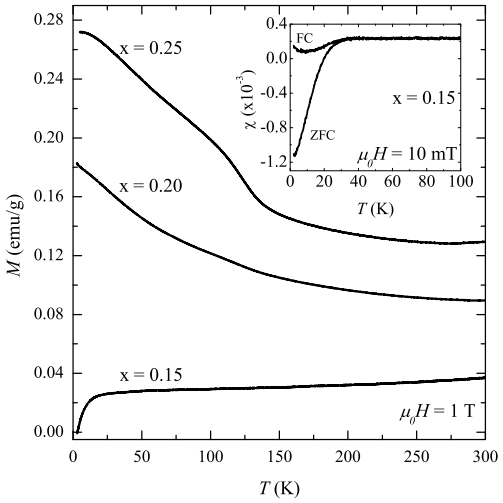

FIG. 3: Magnetization M of $Ca_{1-x}La_xFe_2As_2$ with x = 0.15, 0.20, and 0.25 measured with magnetic field perpendicular to the c axis of the single crystals. The inset shows χ under field cooled and zero-field cooled conditions for $Ca_{0.85}La_{0.15}Fe_2As_2$.

To further investigate $Ca_{1-x}La_xFe_2As_2$, specific heat measurements were executed. Example data for $Ca_{0.85}La_{0.15}Fe_2As_2$ are shown in Figure 4. The specific heat is a smooth function of T and reaches approximately 120 J/mol K at 300 K, which corresponds well with the expectation from classical physics of about 24.9 J/mol K for each atom in $Ca_{0.85}La_{0.15}Fe_2As_2$. The electronic contribution was found by fitting to $C_P = \gamma T + \beta T^3$ power

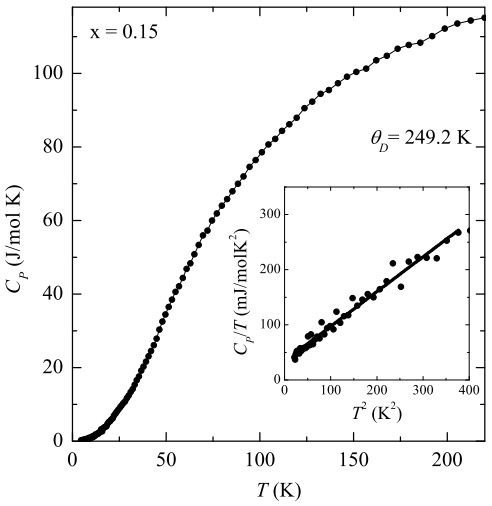

FIG. 4: Specific heat versus temperature ($C_P(T)$) for $Ca_{0.85}La_{0.15}Fe_2As_2$. Inset shows the C_P/T versus T^2 below 20 K.

law for 400 K$^2 \geq T^2 \geq$ 20 K^2 with γ= 32 mJ/mol K^2 and β= 0.64 mJ/mol K^4; these values and our estimate of of Debye temperature (θ_D = 249.2 K) are close to those of similar compounds.[12] The behavior of the specific heat for x = 0.20 and 0.25 is similar.

IV. THERMAL EXPANSION MEASUREMENTS

The linear TE normalized to the length at 300 K, $\triangle L/L_{300}$, along the a and c axes is presented in Fig. 5 for $Ca_{1-x}La_xFe_2As_2$ with x = 0.15, 0.20, and 0.25. Focusing on panel (b) for x = 0.20 along a, $\triangle L/L_{300}$ decreases dramatically with increasing temperature. The magnitude of variation of $\triangle L/L_{300}$ between 5 K and 300 K is 6.7×10^{-3}, which is significantly larger than elemental metals like Mg (4.6×10^{-3}), Al (4.1×10^{-3}) and Cu (3.2×10^{-3}), all of which have large *but* positive TEs.[1] Along the c direction, $\triangle L/L_{300}$ decreases with increasing temperature from 5 K to 98 K and thereafter increases with further increasing temperature. The magnitude of the maximum in $\triangle L/L_{300}$ along a (6.7×10^{-3} near 5 K) is higher than that of c (4.8×10^{-3} near 98 K). The behavior of the x = 0.15 sample is similar (Fig. 5(a)), but x = 0.25 (Fig. 5(c)) exhibits a weaker $\triangle L/L_{300}$ along a and a remarkably strong *expansion* along c. Insets in Fig. 5 display the volume TE, $\triangle V/V_{300}$, as a function of temperature. It is strongest for x = 0.15, with $\triangle V/V_{300}$ exhibiting a dramatic decrease of 14×10^{-3} upon heating from 5 K to 300 K. The effect is weaker, about 10×10^{-3} for x = 0.20, with the formation of a minimum near 237 K. In the case of x = 0.25, the minimum has moved down to 156 K, and the change in $\triangle V/V_{300}$ is smaller with nearly identical volumes at the endpoints of 5 K

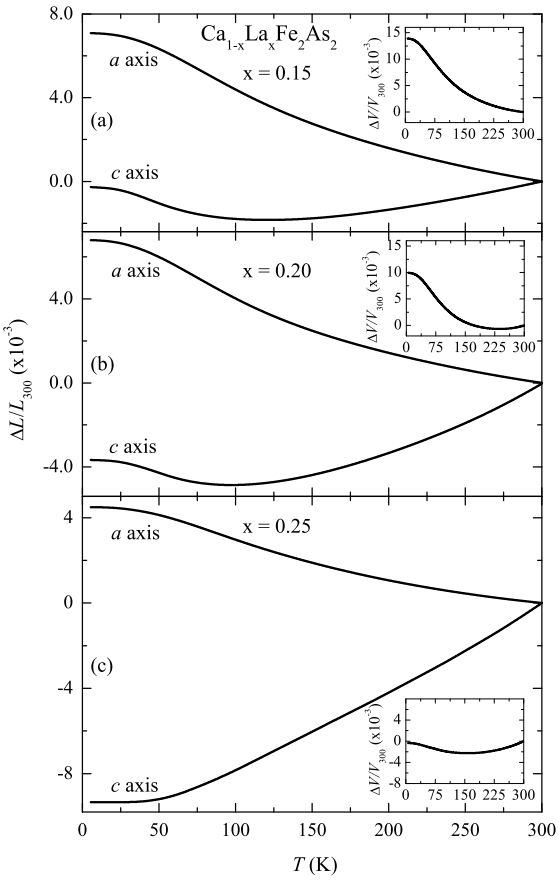

FIG. 5: Linear thermal expansion $\triangle L/L_{300}$ along the a and c axes for $Ca_{1-x}La_xFe_2As_2$. Data were acquired at 0.2 K intervals. The insets reveal the volume thermal expansions $\triangle V/V_{300}$.

and 300 K.

The c-axis linear TE values reported here are significantly smaller in the 5 K to 300 K temperature range than those observed for a x = 0.19 sample.[6] In that case $\triangle L/L_{300}$ along the c axis was found to be 34×10^{-3}. This value is more than 3 times larger than the c-axis thermal expansion observed in any of our samples. We believe that the discrepancy is associated with the fact that Ref. 6 determined the c-axis lattice parameter in their temperature dependent measurement from a single diffraction peak. However, the object in that work was *not* to measure the thermal expansion, and as such, no discussion of temperature-dependent calibration or resolution in determining the lattice parameter was provided.[13]

The linear thermal expansion coefficients α_a and α_c for the a and c axes, respectively, are shown in Fig. 6. These were determined by taking the temperature derivatives of the data in Fig. 5 (i.e. $\alpha = (1/L_{300K})(\partial \triangle L/\partial T)$). While α_a is negative over the entire measured temperature range for all three samples, its magnitude is significantly smaller for x = 0.25. The behavior of α_c is quite similar for x = 0.15 and 0.20, but dramatically different for x = 0.25 for which no negative TE is observed along

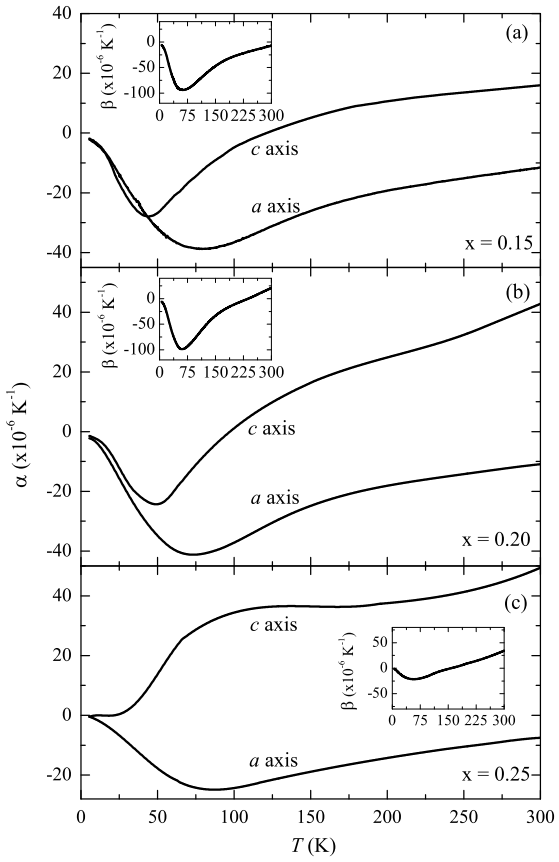

FIG. 6: Linear thermal expansion coefficient ($\alpha = (1/L_{300K})(\partial\triangle L/\partial T)$) along the a and c axes for $Ca_{1-x}La_xFe_2As_2$. The insets reveal the volume thermal expansion coefficients β.

c. The magnitudes of α are extremely large, reaching values of 41×10^{-6} K^{-1} at 73 K and 24×10^{-6} K^{-1} at 49 K for a and c, respectively for x = 0.20. For all samples, the magnitudes of α along both axes decrease as the temperature approaches 0 K, suggesting compliance with the third law of thermodynamics. The volume thermal expansion coefficient β (insets of Fig. 6) were calculated by taking the temperature derivatives of $\triangle V/V_{300}$; β exhibits minima in all three cases, but the magnitude of the minimum and the overall magnitude is dramatically smaller for x = 0.25. Normally, discontinuities in α and β at T_c would be expected[14] for a superconductor at the 2nd-order normal-superconductor phase transition. However, no indication of superconductivity is observed due to the low superconducting volume fractions.

V. DISCUSSION AND CONCLUSIONS

Narrow regions of large, NTE resulting from phase transitions are not uncommon in nature, but smooth, broad regions as revealed in Figs. 5 and 6 are very unusual.[15] Inspection of the electrical resistivity and magnetic susceptibility data (Figs. 2 and 3) show no indication of a phase transition. Heat capacity was also measured to search for a phase transition, but none was observed (see Fig. 4). The Grüneisen parameter $\gamma_G = \beta BV/C_V$ was estimated for $Ca_{0.85}La_{0.15}Fe_2As_2$, under the assumption that the constant pressure specific heat C_P is approximately equal to the constant volume specific heat C_V. The bulk modulus B was calculated from measurements of the lattice parameters[16,17] under pressure at ∼45 K and 300 K, and using our β and C_P data for x = 0.15, we found γ_G(300 K) ≈ 1.0 and γ_G(45 K) ≈ -22. The large, negative value near 45 K is reflective of the presence of anomalous phonon modes, which are the likely source of the unusually large, negative thermal expansion as well as the peculiar temperature dependencies of α and β in the 50 K to 150 K temperature range.

The TE in the present sample is very unusual compared to the behavior observed in closely-related materials. For example, α is positive along all crystallographic directions over the entire temperature range for $CaFe_2As_2$, except for the region including the tetragonal-orthorhombic phase transition; the same is true[18] for $SrFe_2As_2$ and $BaFe_2As_2$. For samples where the tetragonal-orthorhombic phase transition is suppressed by Co-doping for Fe, α also remains positive except for the region near and below the superconducting phase transition, where α is only slightly negative along both axes.[14,19] Furthermore, the Co-doped samples exhibit the largest α values along c, with α_a a factor of ∼4 smaller.[14] These comparisons point toward La doping as playing an important role in the anomalous TE.

Recent experiments[6] have shown that doping of rare earth elements La, Ce, Pr, or Nd for Ca in $CaFe_2As_2$ suppresses the tetragonal-orthorhombic phase transition. For Pr and Nd doping, a phase transition to the collapsed-tetragonal phase occurs near 50 K and modest pressures of 0.05 GPa and 0.35 GPa are required to drive $Ca_{0.78}Ce_{0.22}Fe_2As_2$ and $CaFe_2As_2$ into the collapsed-tetragonal phase, respectively;[6,8] this phase transition in the Pr- and Nd-doped samples is accompanied by a dramatic increase in the number of itinerant-charge carriers.[6] Electronic band structure calculations[7] for $CaFe_2As_2$ reveal a dramatic dependence of the c-axis lattice parameter on the magnetic moment. Furthermore, La doping was recently shown to bring $CaFe_2As_2$ close to the collapsed-tetragonal phase boundary, but it does not induce the phase transition as the smaller rare-earth dopants do.[6] These combined observations indicate that the lattice, electronic and magnetic degrees of freedom are strongly coupled in $CaFe_2As_2$, and that it resides near a structural phase instability. The observation that La doping (x = 0.15 and 0.20) leads to unusual behavior in the thermal expansion, and further doping (x = 0.25) alters that behavior in a dramatic fashion, lends support to the existence of a structural instability in $CaFe_2As_2$.

Since the TE is normally dominated by lattice vibrations through the majority of the temperature range of our measurements, they must be at the source of the

unusual behavior of α and β in $Ca_{1-x}La_xFe_2As_2$. However, lattice vibrations are directly influenced by the electronic potentials within which the atoms reside. The strong coupling among lattice, electronic, and magnetic degrees of freedom must play a significant role in modifying these electronic potentials in $Ca_{1-x}La_xFe_2As_2$. In fact, measurements and calculations of phonon dispersion in $CaFe_2As_2$ reveal unusual broadening that is absent in $BaFe_2As_2$, presumably due to the close proximity of $CaFe_2As_2$ to the collapsed-tetragonal phase.[20] Since La-doping for Ca in $CaFe_2As_2$ moves this system yet closer[6] to the boundary with the collapsed-tetragonal phase, it is likely to enhance anomalous behavior in the phonon dispersion. This could lead to the development of anharmonic lattice vibrations that are atypical for solids, these anomalous vibrations would be the consequence of electronic and magnetic instabilities that are strongly coupled to the lattice. For example, quartic contributions to the phonon potential[3] clarify the NTE observed[21] in ScF_3.

NTE is observed in a number of inorganic compounds and non-metallic elements. Selenium ($\alpha_a >$ 69.8×10^{-6}K^{-1}, $\alpha_c >$ -13.4×10^{-6} K^{-1}, and $\beta >$ +125×10^{-6}K^{-1} at 300 K) and Tellurium ($\alpha_a >$ 29.6×10^{-6}K^{-1}, $\alpha_c >$ -2.3×10^{-6} K^{-1}, and $\beta >$ +57×10^{-6}K^{-1} at 293 K) exhibit modest NTEs along one axis.[1] Below ∼100 K ZnO exhibits[1] NTE ($\alpha_a >$ -0.5×10^{-6}K^{-1}, $\alpha_c >$ -0.9×10^{-6} K^{-1}, and $\beta >$ -1.9×10^{-6}K^{-1}). Low-frequency optical modes lead to NTE in the AB_2O_8 materials, such as the cubic compound[15,22,23] ZrW_2O_8, which exhibits $\triangle V/V_{300}$ about 25% smaller in magnitude than $Ca_{0.80}La_{0.20}Fe_2As_2$ from 5 K to 300 K. The linear thermal expansion coefficients of the anisotropic compound $LiAlSiO_4$ in the region[24] 200 K to 800 K nearly cancel one another to yield $\beta <$ 1×10^{-6} K^{-1} ($\alpha_a \approx$ 8.1×10^{-6} K^{-1} and $\alpha_c \approx$ -15.4×10^{-6} K^{-1}). Cubic siliceous faujasite[25] reaches a value of α = -4.2×10^{-6} K^{-1}. $AlPO_4$-17 exhibits an exceptionally large volume thermal expansion coefficient[26] of β = -35×10^{-6} K^{-1}, composed of comparable values of α_a and α_c, which is nearly a factor of 3 smaller in magnitude than the value shown in the inset of Fig. 6b. The $Sc_2W_3O_{12}$ family is known to exhibit NTE, with the strongest[27] volumetric effect of -20×10^{-6} K^{-1} in $Lu_2W_3O_{12}$. This value is composed of α_a = -9.9×10^{-6} K^{-1}, α_b = -2.2×10^{-6} K^{-1} and α_c = - 8.3×10^{-6} K^{-1}. The magnitudes and temperature dependencies of α_a, α_c and β in $Ca_{1-x}La_xFe_2As_2$ place their TEs among some of the largest NTEs observed among inorganic materials. In addition, unlike the aforementioned materials, they are metallic.

Large and sometimes NTEs are observed in organic materials. For graphite, β is positive, but it is composed of positive and negative α values[1] ($\alpha_a >$ -1.2×10^{-6} K^{-1} and $\alpha_c <$ 27×10^{-6} K^{-1}). The cubic compounds[28] $CdPt(CN)_6$ and $Zn(CN)_2$ exhibit α = -10.0×10^{-6} K^{-1} and α = -17.4×10^{-6} K^{-1}, respectively. Molecular framework materials exhibit large volumetric NTE. These include a dumbbell-shaped organic molecule[29] ($\alpha_a = 515 \times 10^{-6}$K^{-1}, $\alpha_b = -85 \times 10^{-6}$K^{-1}, $\alpha_c = -204 \times 10^{-6}$K^{-1}, and $\beta = 47 \times 10^{-6}$K^{-1}), the frame work material[30] $Ag_3[Co(CN)_6]$ ($\alpha_a = 150 \times 10^{-6}$K^{-1}, $\alpha_c = -130 \times 10^{-6}$K^{-1} and $\beta = 170 \times 10^{-6}$K^{-1}), the cubic single-network compound[31] $Cd(CN)_2$ ($\alpha_a = -33.5 \times 10^{-6}$K^{-1} and $\beta = -100 \times 10^{-6}$K^{-1}), $Zn_{0.64}Cd_{0.36}(CN)_2$ framework materials[32] ($\beta = -60 \times 10^{-6}$K^{-1}). The volumetric thermal expansion of $Ca_{0.85}La_{0.15}Fe_2As_2$ and $Ca_{0.80}La_{0.20}Fe_2As_2$ are as large or larger in magnitude than most of these, and their negative α_a values are within the range of many of the negative α values of these comparison materials. Note that most of the values for α and β in the studies mentioned above for organic and inorganic materials were obtained through use of diffraction techniques, which generally do not reveal the temperature dependencies of α as shown in Fig.6 because of the large spacing in temperature between neighboring lattice parameter values.

Most materials exhibiting NTE are insulators. $Ca_{1-x}La_xFe_2As_2$ is a metal that exhibits an extraordinarily large NTE that is not observed in related Fe-As compounds. Its close proximity to a structural phase instability involving strong coupling among lattice, electronic, and magnetic degrees of freedom is the likely source of the unusual behavior. This study reveals large, NTE as another potentially important property of the Fe-As materials that are currently under intense investigation for their superconducting properties.

This material is based on the work supported by the National Science Foundation under Grant No. DMR-0907036.

[1] T. H. K. Barron and G. K. White, *Heat Capacity And Thermal Expansion At Low Temperatures* (Kluwer Academic/Plenum, New York, 1999).

[2] G. D. Barrera, J. A. O. Bruno, T. H. K. Barron, and N. L. Allan, J. Phys.: Condens. Matter **17**, R217 (2005).

[3] C. W. Li, S. Tang, J. A. Muñoz, J. B. Keith, S. J. Tracy, D. L. Abernathy, and B. Fultz, Phys. Rev. Lett. **107**, 195504 (2011).

[4] G. Schwarz, Cryogenics **28**, 248 (1988).

[5] A. I. Goldman, D. N. Argyriou, B. Ouladdiaf, T. Chatterji, A. Kreyssig, S. Nandi, N. Ni, S. L. Bud'ko, P. C. Canfield, and R. J. McQueeney, Phys. Rev. B **78**, 100506(R) (2008).

[6] S. R. Saha, N.P. Butch, T. Drye, J. Magill, S. Ziemak, K. Kirshenbaum, P.Y. Zavalij, J.W. Lynn and J. Paglione, Phys. Rev. B **85**, 024525 (2012).

[7] T. Yildirim, Phys. Rev. Lett. **102**, 037003 (2009).

[8] W. Yu, A.A. Aczel and T.J. Williams, Phys. Rev. B **79**, 020511(R) (2009).

[9] Z. Gao, Y. Qi, L. Wang, D. Wang, X. Zhang, C. Yao, C. Wang and Y. Ma, Europhys. Lett. **95**, 67002 (2011).

[10] Y. Qi, Z. Gao, L. Wang, D. Wang, X. Zhang, C. Yao, C. Wang and Y. Ma, Supercond. Sci. Technol. **25**, 045007 (2012).

[11] J. J. Neumeier, R. K. Bollinger, G. E. Timmins, C. R. Lane, R. D. Krogstad, and J. Macaluso, Rev. Sci. Instrum. **79**, 033903 (2008).

[12] N. Ni, S. L. Bud'ko, A. Kreyssig, S. Nandi, G. E. Rustan, A. I. Goldman, S. Gupta, J. D. Corbett, A. Kracher, and P. C. Canfield, Phys. Rev. B **78**, 014507 (2008).

[13] The lower panels of Fig. 4 in Ref. 6 show the peak intensities versus temperature in contour plots for the (110) and (006) diffraction peaks for x = 0.19. The (006) peak widths correspond to about 0.25 Å or about 2% for the c lattice parameter. For comparison, our x = 0.20 sample exhibits $\triangle L/L_{300}$ of 0.47% between 125 K and 300 K along c.

[14] M. S. da Luz, J. J. Neumeier, R. K. Bollinger, A. S. Sefat, M. A. McGuire, R. Jin, B. C. Sales, and D. Mandrus, Phys. Rev. B **79**, 214505 (2009).

[15] T. A. Mary, J. S. O. Evans, T. Vogt, and A. W. Sleight, Science **272**, 90 (1996).

[16] R. Mittal, R. Heid, A. Bosak, T. R. Forrest, S. L. Chaplot, D. Lamago, D. Reznik, K.-P. Bohnen, Y. Su, N. Kumar, S. K. Dhar, A. Thamizhavel, Ch. Rüegg, M. Krisch, D. F. McMorrow, Th. Brueckel, and L. Pintschovius, Phys. Rev. B **81**, 114502 (2010).

[17] A. Kreyssig, M. A. Green, Y. Lee, G. D. Samolyuk, P. Zajdel, J. W. Lynn, S. L. Bud'ko, M. S. Torikachvili, N. Ni, S. Nandi, J. B. Leão, S. J. Poulton, D. N. Argyriou, B. N. Harmon, R. J. McQueeney, P. C. Canfield, and A. I. Goldman, Phys. Rev. B **78**, 184517 (2008).

[18] S. L. Bud'ko, N. Ni, and P. C. Canfield, Philos. Mag. **90**, 1219 (2010).

[19] S. L. Bud'ko, N. Ni, S. Nandi, G. M. Schmiedeshoff, and P. C. Canfield, Phys. Rev. B **79**, 054525 (2009).

[20] R. Mittal, L. Pintschovius, D. Lamago, R. Heid, K-.P. Bohnen, D. Reznik, S. L. Chaplot, Y. Su, N. Kumar, S. K. Dhar, A. Thamizhavel, and Th. Brueckel, Phys. Rev. Lett. **102**, 217001 (2009).

[21] B. K. Greve, K. L. Martin, P. L. Lee, P. J. Chupas, K. W. Chapman and A. P. Wilkinson, J. Am. Chem. Soc. **132**, 15496 (2010).

[22] R. Stevens, J. Linford, B. F. Woodfield, J. Boerio-Goates, C. Lind, A. P. Wilkinson, and G. Kowach, Chem. Thermodyn. **35**, 919 (2003).

[23] Z. Schlesinger, J. A. Rosen, J. N. Hancock, and A. P. Ramirez, Phys. Rev. Lett. **101**, 015501 (2008).

[24] N. Khosrovani and A. W. Sleight, Int. J. Inorg. Mat. **1**, 3 (1999).

[25] M. P. Attfield and A. W. Sleight, Chem. Commun. **5**, 601 (1998).

[26] M. P. Attfield and A. W. Sleight, Chem. Mater. **10**, 2013 (1998).

[27] P. M. Forster, A. Yokochi, and A. W. Sleight, J. Sol. State Chem. **140**, 157 (1998).

[28] K. W. Chapman, P. J. Chupas, and C. J. Kepert, J. Am. Chem. Soc. **128**, 7009 (2006); K. W. Chapman and P. J. Chupas, ibid. **129**, 10091 (2007).

[29] D. Das, T. Jacobs, and L. J. Barbour, Nature Mater. **9**, 36 (2010).

[30] A. L. Goodwin, M. Calleja, M. J. Conterio, M. T. Dove, J. S. O. Evans, D. A. Keen, L. Peters, and M. G. Tucker, Science **319**, 794 (2008).

[31] A. E. Phillips, A. L. Goodwin, G. J. Halder, P. D. Southon, and C. J. Kepert, Angew. Chem. Int. Ed. **47**, 1396 (2008).

[32] A. L. Goodwin and C. J. Kepert, Phys. Rev. B **71**, 140301 (2005).